Application of Markov chain and entropy analysis to lithologic succession- An example from the Post-Rift Cretaceous and Tertiary Formations, Kombe-Nsepe area, Douala Subbasin, Cameroon

[1]Dinga Elvis Tita and [2]Adrien Lamire Djomeni

[1]Department of Geology, University of Buea, Cameroon. BP.63. Buea
[2]Department of Earth Sciences, Faculty of Sciences, University of Douala Cameroon.

Abstract- The arrangement of lithofacies of the Cretaceous and Tertiary Formations of the Kombe-Nsepe area southeastern part of the Douala sub basin has been examined by statistical techniques. A statistical approach by a modified Markov process model and entropy function is used to prove that the Formations of the Kombe-Nsepe area developed distinct cyclicities during deposition. The lithologies have been condensed into five facies states viz. Dark/grey shale, inter-bedded fine grained sandstone and shale, coarse to medium-grained sandstone, conglomerate faciesand carbonate and argillaceous shale for the convenience of statistical analyses. Markov chain analysis indicates the arrangement of lithofacies in form of fining upward cycles. A complete fining upward cycle consists of conglomerate or coarse-grained sandstone at the base sequentially succeeded by medium-and fine grained sandstones, inter-bedded fine grained sandstone and shale, and carbonate and argillaceous shale at the top. The chi-square stationarity test implies that these cycles are stationary in space and time. The cycles are interpreted in terms of in-channel, point bar and overbank facies association in a fluvial-alluvial system. The randomness in the occurrence of facies within a cycle is evaluated in terms of entropy, which has been calculated from the Markov matrices. Two types of entropies are calculated for every facies state; entropy after deposition *E*(post) and entropy before deposition *E*(pre), which together form entropy set; the entropy for the whole system is also calculated. These values are plotted and compared with Hattori's idealized plots, which indicate that the sequence is essentially asymmetrical cycle (type A-4 of Hattori). The asymmetrical cyclical deposition of the post-rift Cretaceous and Tertiary Formations is explained by the lateral migration of stream channels in response to varying discharge and rate of deposition across the alluvial plain.

Index Terms- Douala sub basin, Entropy analysis, lithologic succession, Markov matrices

I. INTRODUCTION

THe Douala/Kribi-Campo (DKC) basin constitutes one of a series of continental shelf basins extending in West Africa from the edge of the Niger delta in Cameroon to the Walvis ridge near the Angola–Namibia border. It comprises of the Early Cretaceous to Tertiary series which are common in West Africa basins. Theseseries are the main hydrocarbons bearing sedimentary succession of the DKC basin.According to [1], the DKC Basin is sub dividedinto two sub basin; the Douala sub basinto the north and the Kribi-Campo sub basin to the south. The present study is centre on the Douala sub basin (DSB).Since the first exploration activity in the 1950's which resulted in the Soualaba-1(SA-1) discovery, many wildcats have been drilled in the Kombe-Nsepe area (KNA)southeastern part of the DSB generating voluminous data (cuttings, cores, well logs etc) on the subsurface geology. These data have been mostly used for hydrocarbons exploration activities (only unpublished industry reports as literature have been available for the area). The study area is basically made up of swamps with no visible outcrop (Fig.1) hence the origin; depositional setting and stratigraphic attribution of the sediments in the area before now were poorly understood.

Numerous studies have shown that sedimentary sequences contain varietal assemblages of facies which are commonly cyclic and characteristic of particular sedimentary environments [2, 3, 4 and 5].However vertical variations of lithofacies within a given sequence play an important role in the recognition of depositional environment and their lateral dispersal. It is of particular importance in the context of the widely accepted law of the correlation of facies as proposed by [6] and elaborated by [7, 8 and 9] and recently by [10]. Gradual transition from one facies to another implies that the two facies represent environments that once were adjacent laterally.

In a depositional environment, the physical processes and random events usually advance side by side and as a result produce intricate patterns in lithologic successions observed in outcrops. It is appropriate therefore that sedimentary succession at individual localities be tested for such cyclic order on an objective and quantitative basis [11]. Examination of the well logs in the KNA indicates the repetitive occurrence of different lithologies. Although, individual cycles are present, the scarcity of comprehensive exposures due to weathering makes it difficult to determine regional distribution of cyclicity. Hence, information obtained from 15 wells from the KNA, penetrating the Cretaceous section providing a precise record of lithologic transitions has been utilized for various statistical analyses.In order to determine the depositional architecture and its regional variations a check of the results obtained so far [12, 13, 14 and 15] by mathematical meansis desirable. The vast amounts of data

obtained through counting of lithologic transitions of well logs justify the application of Markov chain and entropy functions. The objectives of the present study are:

-To deduce lithologic transitions in vertical sequences through space and time;

-To evaluate the degree of ordering of lithofacies using entropy functions;

-To recognize the broad depositional environment of the post-rift Cretaceous and Tertiary Formations in the KNA.

II. General Geology

The DSB belongs to a set of basin located on West African margin which run from Angola to Cameroon. It is located 3°20 N to 5°N and 9° E to 10°30' E (Fig. 1), covering a total surface area of 12,805 sq. km. It has a crescent shape starting from the south-eastern border of Mount Cameroon and extends throughout the Atlantic coast with a gradual decrease in width of the onshore part towards the South of the sub basin up to the North of Kribi Campo sub basin. The DSB is bounded to the W and NW by the Cameroon Volcanic Line (CVL) which is superimposed on the Central Africa Shear Zone (CASZ) and represents its limit with the Rio Del-Rey basin to the South by the Kribi Fracture Zone (KFZ) which delimits the Kribi-Campo sub-basin. Eastward, the boundary is the Precambrian basement. The onshore part of the DSB has a trapezoic shape and covers a total surface area of about 6955sq.km while the offshore part covers an area of about 5850 sq.km.

The tectonic evolution of the DSB was studied by [16] and related it to the history of the West African margin which presents three major stages:

1) The first stage begins with the Precambrian phase of cratonisation, granitisation and sedimentation which was followed by the pan-africanorogenesis.

2) After this Cambrian phase, the geology of the DSB is only known starting from the lower Cretaceous during which epicontinental sedimentation begins to field an afro-brazilian depression. Sediments whose age varies from Cretaceous to Pliocene are discordant on the Precambrian pan-african basement (**Table 1**). The sedimentation was accompanied by Plutonism (Cenomanian) and volcanism (Miocene) which products cover sediments in some area (like volcanic products of Mount Cameroon).

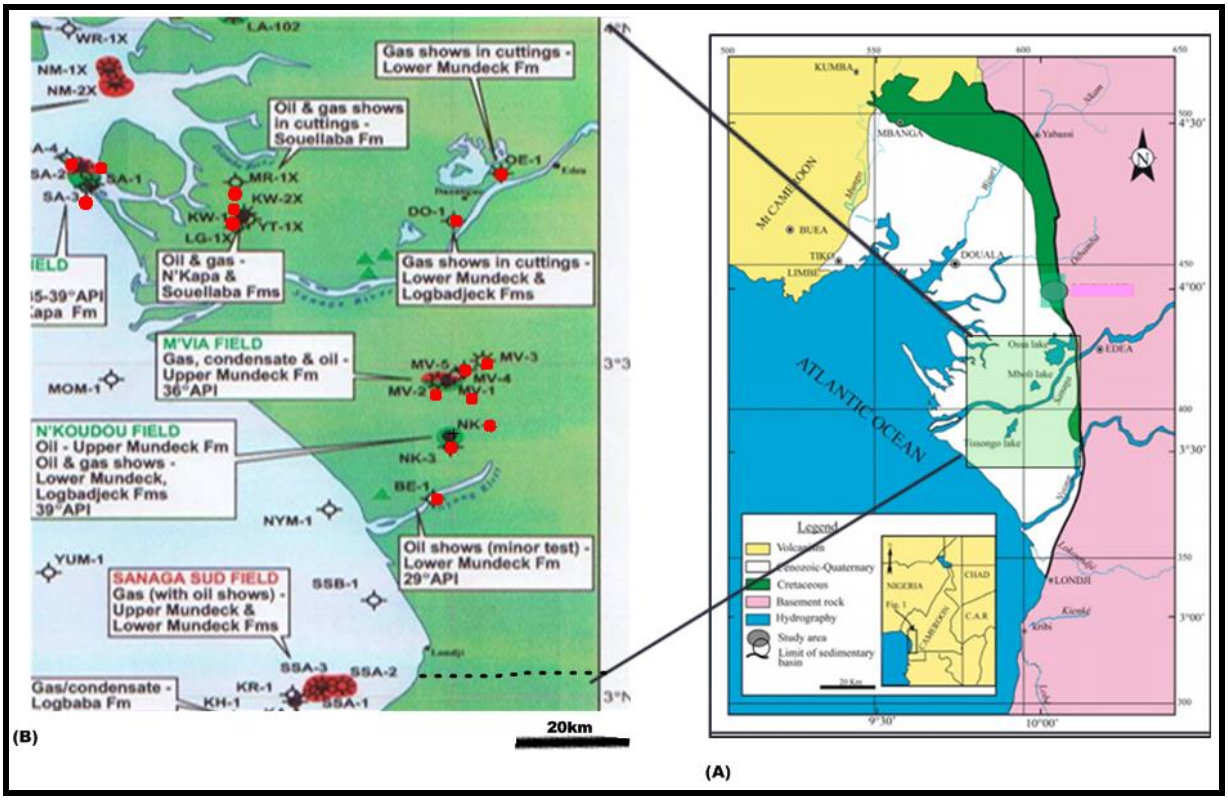

Fig.1. A) Map of CameroonShowing the Location of the sub basin, B) Location map of study area showing the locations of the representativewellused for the presentstudy in red.

The complete tectono-lithostratigraphic sequence represented in Table 1 is based on oil exploration seismic and drill data offshore and comprises seven formations from the barremian-Aptian to present deposited during the pre-rift, syn-rift, rift-drift and post-rift basin phases.

1) Pre-rift phase: According to [17] Jurassic continental sediments were deposited in an afro-brasilian depression, an intracratonic sag basin that extended over the Gabon and Douala basins prior to the rifting of the Afro-American plate.

2) Rifting phase (Jurassic-Barremian): According to [17] the stratigraphic sequence formed during the rifting phase appears to be controlled by listric faulting and associated roll over anticlines.

3) The syn-rift phase was responsible for the fracture pattern which is closely controlled by inherited structures of the Precambrian basement. This phase is characterized by an intensive erosion activity of the highlands and deposition in graben previously formed. In the Kribi/Campo sub- basin, these units are named Lower Mundeck[13, 18 and 19], and are shallowly buried by younger sediments [20]. They are made up of conglomerates, conglomeratic sandstones, organic matter-rich dark marls interbedded with thin limestones and black to dark grey shales. In the DSB, Aptiansyn-rift deposits overlie a narrow bench of attenuated continental basement [11 and 21]. Here, they are referred to as the upper Mundeck Formation.

The upper Mundeck Formation are made up of continental polygenic conglomerates with arkosic sandstones cement showing rare interbedded ferruginous clay, an alternation of laminated silt or sand with black shales and arkosic medium grain sandstones[18]. Their environments of deposition have been interpreted (on a regional bases) as ranging from terrestrial to lacustrine, through restricted to fully marine. Pre-Aptiansyn-rift deposits and basement rocks have not been reached by drilling.

Table 1. Stratigraphic Column showing the seven Formations of the Douala sub basin Adopted from Lawrence *et al*., (2002)

Age (Ma)	*Chronostratigraphy*			*Formations*	*Techtono-stratigraph*
	Tertiary	*Neogene*	*Pleistocene*	*Wouri*	*Drift 111*
			Pliocene	*Matanda*	
10			*Miocene*	*Souellaba*	
20					
		Paleogene	*Oligocene*		*Drift 11*
30					
40			*Eocene*	*Nkapa*	
50					
60			*Paleocene*		
70	*Mesozoic*	*LateCretaceous*	*Maastrichtian*	*Logbaba*	
80			*Campanian* *Santonian* *Coniacian*		*Drift 1*
90			*Turonian* *Cenomanian*	*Logbadjeck*	
100		*EarlyCretaceous*	*Albian*	*UpperMundeck*	
110					
120			*Aptian*	*LowerMundeck*	*Transition*
					Rift 111
130			*Neocomian*	*Basement*	*Rift 11*
140			*Barremian*		*Rift 1*
150		*Jurassic*			
	Precambrian				

4) The rift-drift transition phase (mid-late Aptian).

This phase was marked by salt deposition and the transform directions resulting in a series of cross-faults which have segmented the rift structure [22]. This phase of basin evolution is poorly preserved in the DSBand only one well drilled in the basin has reached the top of a salt unit [11, 17 and 23]. Aptian salt is absent (if ever deposited) to the north and eastern part of the basin, due to an end Aptian/early Albian uplift, which resulted in the lower Mundeck Formation being unconformably overlain by the upper Mundeck Formation from which they are separated by a probably breakup unconformity [21 and 24].This fact help to suggest that salt was deposited in the final stage of continental rifting. In the DSB, evidence of evaporites has not yet been well stated.

5) Post-rift phase (Albian-Present): Following salt deposition, post-rift sedimentation in the DKC basin was dominated by marginal to clastic sedimentation, with shallow water carbonate deposition occurring as sporadic build ups between the Albian and Paleocene. From Albian to Turonian, the juvenile South Atlantic Ocean was filled with anoxic bottom

waters presumably caused by restriction of open ocean circulation and ponding of bottom waters between Walvis Ridge and Rio Grande Rise in the South, and equatorial fracture zone topography in the North[25 and 26]. According to [27] compressive deformation has also occurred in Cretaceous/Tertiary deposits in several places both along and near the African margin. Older structures, especially the cross-faults, were reactivated by transpressional stresses, resulting in a folding and faulting deformation. According to [26], the post-rift phase comprises three stages of drift:

a) The first drift stage was from Albian-Coniacian and is characterized by rotational fault blocks in the proximal part, salt movement and gravity sliding [17 and 27]. These structures are linked to gravitational instability of the margin and the presence of salt. Sedimentologically, this phase is marked in the DKC basin by a major regression leading to the decrease of the sea level. The consequence was the erosion of the Lower Cretaceous sequence thereby creating a surface of unconformity with an irregular topography. The unconformity at the base of upper Cretaceous was followed by the deposition of the Logbadjeck formation (Cenomanian- Coniacian).

b) The second drift phase named Drift II (Campanian to **Oligocene)** was a discrete drift which is linked to regional tectonic episode. The Logbaba (Cenomanian-Maastrichtians) and the Nkapa (Paleocene-Eocene) formations were deposited during this phase. Also during this phase, original rift-related structures were inverted and the platform sedimentary section was folded [15].The Santonian unconformity separating the first and second drift stages is recognized along the West African margin as a result of the uplift during the Cretaceous episode[22]

c) The third drift stage (Miocene) named drift III has been linked to gravity sliding caused by uplift in the Tertiary. The Uplift and erosional unconformity are dated to about 30 - 40 Ma. This phase in the DSB was marked by deposition of the Souellaba formation(Oligocene), the Matanda formation (Miocene) and Wouri formation (Pliocene-Pleistocene).

The areas considered in thepresent work constitute the southeastern border of the DSB (Fig.1B). It covers a total surface area of 3026sq.Km and it is mostly onshore with some shallow offshore acreage (water depth < 10m) in the southwest which is part of the Cameroon Estuary. The sedimentary series known here are Early Albian to Pleistocene in age according to [22] and thus belong to the upper Mundeck, Logbadjeck, Logbaba, Souellaba, Matanda and Wouri Formations.

III. Data sets and Methods of study

3.1 Data sets

In view of the non-availability of good vertical sections in the KNA, the vertical lithofacies relationshipof Formationsin the areabefore now could not beestablished. Since the stratahave no outcrop in the area studied, the present investigationis based entirely on the data derived fromwell logs. A total of 15boreholes logs (MV-1, MV-2, MV-3, MV-4, OE-1, DO-1, NK-2, NK-3, BE-1, LG-1, KW-1, KW-2, SA-1, SA-2, and SA-3), fromlocalities scattered throughout the area (Fig.1B)are used.

Owing to the disagreement among different workers regarding the scale and boundary of a sedimentary cycle [28] proposed that a sedimentary cycle commences at the base of coal seam or shalewhereas[29] gave a formation status to each cycle with sandstone at the base. According to [30] the minimum thickness of a sedimentary cycle is 0.3 m, but [31] assigned it 1m), the sequence of strata of 1m and above in thickness with basal coarse member (conglomerate or sandstone) and terminating with shale bed or carbonaceous shale has been considered to constitute a cycle in the present work. This is in conformity with the definition of fining upward cycle of [32] for the alluvial sediments and coal cycle of [31]. Both types represent complete cycles of stream regime in fluvial environment in conformity with the concept of [33].

For simplicity of analysis and to avoid the risk of error, the lithologies named in the end of well report's and observed from the well logs were condensed into five facies states on the basis of lithology and texture as observed in the well records. To analyze cyclic characters through spaceand time, the lithofacies transitions are analyzedseparately in each borehole log, and by pooling thedata for three major age groups (lower Cretaceous, upper Cretaceous and Tertiary) as well as for the entire study area.

The five facies are:

- Facie **A**: Dark/grey shale
- Facie **B**: Inter-bedded fine-grained sandstone and shale that includes parallel and ripple-drift cross-laminated medium to fine grained sandstones
- Facie **C**: Medium to coarse-grained sandstone that includes trough- and tabular cross-bedded coarse to medium- and medium-grained sandstones.
- Facie **D**: Coarse-grained sandstone that includes massive conglomerate, trough cross-bedded pebbly sandstone, and flat bedded coarse-grained sandstone, trough and tabular cross-bedded coarse-grained sandstones.
- Facie **E**: Carbonate and argillaceous shale

Condensation of lithologies into the above five lithofacies seems reasonable as C and D represent distal- and mid-channel bars deposit respectively; B is characteristic of bar-top and abandoned-channel deposits; A represent proximal flood plain, abandoned channel fill and over bank deposits and E is the deposit in a probable peat swamps[2,33, 34,35,36 and 37].

3.2Methods of study (Analytical Procedures)

From the concept of cycles of sedimentation, the initial state or lithology determine to some extent the subsequent state or lithology. It was from this concept that [38] conceived the idea of using Markov chain as an analytical tool in the study of vertical lithofacies relationship in stratigraphic sequences. According to [39] Markov chain analysis offers an objective approach to model discrete variables such as lithologies or facies. This method also offers a way to compare laterally juxtapositional tendencies of facies to those in vertical sections. For a sequence to possess the first-order Markov property, the rock type at a point "n" depends to some extent on the rock type observed at the proceeding point i.e. n-1[40]. If the lithologic sequence is found to be governed by a Markovian process, the next logical step would be to evaluate the degree of randomness within the Markov chain by using the entropy as proposed by

[41]. The literature on Markov chain and entropy analyses is now rapidly growing. Test cases have been published by[42, 43,44,45,46 and 47].

The method used in this study is based mainly on those of [48 and 49] which have been modified by[46]. In addition, the nature of cyclic order of a sequence is studied using entropy concept following [41].

3.1 Structuring Datafor Markov Chain Analysis

Lithologic transitions, to test the presence or absence of Markov property or lack of it are investigated at major age intervals and at the entire area levels separately using data from 15 well logs. There are basically two methods of structuring data from actuallithologic successions. The first method termed an 'Embedded Markov matrix' [39] and the second termed 'Regular Markov matrix' [50]. In the present study, the embedded Markov matrix is preferred to the regular Markov matrix for the following reasons:

i)The main purpose of the present study is to deduce lithologic transitions in vertical sequences and to evaluate the degree of ordering of lithofacies. Thefixed interval method of counting attaches undue importance to the element of bed-thicknesswhich might mask the actual facies change.

ii) Selecting an appropriate sampling interval is problematic. A large interval will omit thin bedswhile too small an interval will introduce large values along the main diagonal creatingdifficulties for a proper statistical evaluation of ordering in the sequence.

iii) The regular Markov model is applicable to those stratigraphic sequences where the distribution ofbed-thickness of each facies is exponential. Bed–thickness is,however, more commonly distributed log-normally rather than exponentially.

Tally count matrix based on borehole logs numbering for the major age unit is structured. Subsequently, data for all 15 well logs are added and a bulk matrix is structured at entire area level. Data for the bulk tally matrix at major age units and entire study area level are computed separately following themodified Markov process model after [49].The downward facies transition data of the fifteen wells were summed up to form a transition count matrix, which was processed intotransition count, transition probability, random probability,difference matrices (Tables).

3.1.1 Transition Frequency Matrix (F)

As mentioned above, a first- order embedded chain matrix is structured by counting transition from one facies to another, and the resulting frequency matrix will contain zeros along the principal diagonal (Fij =0) where *i, j* corresponds to row and column number.

3.1.2 Upward Transition Probability Matrix (P)

The upward transition probability matrix pertains to the upward ordering of lithologies in a succession is calculated in the following manner: **Pij** = $\frac{Fij}{SRi}$ where SRi is the corresponding row total.

3.1.3 Downward Transition Probability Matrix(Q)

Similar to the upward transition probability of lithologies a downward transition probability (Q matrix) can also be determined by dividing each element of the transition frequency matrix by the corresponding column total, *i.e.*, **Qji** = $\frac{Fij}{SCj}$where SCj is the column total.

3.1.4 Independent Trials Matrix (R)

Assuming that the sequence of rock types was determined randomly an independent trial matrix can be prepared in the following manner : **Rij** = $\frac{C2}{N-C1}$where C1 is the column total of facies state F1, C2 is the column total of facies state F2 , N is the total number of transitions in the system. The diagonal cells are filled with zeros.

3.1.5 Difference Matrix (D)

A difference matrix (Dij = Pij – Rij) is calculated which highlights those transitions that have ahigher or lower probability of occurring than if the sequence were random. By linking positivevalues of the difference matrix, a preferred downward (or upward)path of facies transitions can be constructedwhich can be interpreted in terms of depositional processes that led to this particular arrangementof facies [2 and 34].

3.1.6 Expected Frequency Matrix (E)

It is necessary to construct an expected frequency matrix (E) which will be used to calculate the chi – square tests. The matrix of expected values is given by **Eij = Rij .SRi**.

3.1.7 Tests of Significance

The cyclicity (Markovian property) of facies states has been tested by chi-square statistics

Using the values of *fij*and *Eij*in the expression

$$x^2=\sum_{i=1}^{n}\sum_{j=1}^{n}(fij-Eij)^2/Eij \quad \text{(eq.1)}$$

x^2 yields a statisticswhich is distributed as a chi-squared variablewith $(n-1)^2-n$ degrees of freedom. Thelarger thex^2 value for a given value of *n*, thestronger the evidence in favor of the Markovianmodel of lithologic transition.

3.2. Entropy analysis

The entropy concept which was introduced by [51] is defined in a lithological sense as "the degree of intermixing of end members or the uncertainty in the composition of a system"[52]. The entropy value is maximum when all the components occur in equal proportions. The value approaches zero as a single end member dominates the composition.Methods of calculation of entropy as suggested by [41] and modified by[46], have been largely followed in the present study. According to [41], two types of entropies exist with respect to each lithological state. The first is an upward probability matrix composed of *pij*, which gives the actual probabilities of the transition occurring in the given section and is calculated as:

Pij = $\frac{Fij}{SRi}$where SRi is the corresponding row total. In the *pij*matrix, the row total sums to unity. From this matrix entropy after deposition(*E*(post)) for each lithological state has been calculated using [46] equation (eqn. 2) .

$$E(post) = -\sum_{j=1}^{n}\sum pij \log_2 pij$$ ..... (eq.**2**)

If ***E(post)*** = 0.0, state i is always succeeded by state **j** in the sequence. If **E(post) >0**, state i is likely to be overlain by different states

The second matrix, containing element ***qji***which represents the probability of the given transition being preceded by any other transition and it is given by**qji** $= \frac{Fij}{SCj}$ where SCj is the column total. The column totals in the ***qji***matrix sums to unity. *E* (pre) (i.e., entropybefore deposition) was then calculated following[46] equation (eqn. 3).

$$E(pre) = -\sum_{j=1}^{n}\sum qij \log_2 qij$$ ..... (eq.**3**)

Large E(pre) signifies that i occur independent of the preceding state.

Ei(post) and Ei(pre) together form an entropy set for state and serves as indicators of the variety of lithological transitions immediately after and before the occurrence of i, respectively.The interrelationships of E(post) and E(pre) were used by [41] to classify various cyclic patterns into asymmetric , symmetric and random cycles. The values of E(post) and E(pre) calculated by equations (2) and (3) increases with the number of lithological states recognized. To eliminate this influence, [41] normalized the entropies by the following equation:

$$\boldsymbol{R}\textbf{(pre)} = \frac{E(pre)}{E(max)}$$ ..... (eq.**4**)

$$\boldsymbol{R}\textbf{(post)} = \frac{E(post)}{E(max)}$$ .....(eq.5)

Where $\boldsymbol{E}\textbf{(max)} = -\log_2 \boldsymbol{1/(n-1)}$, which denotes the maximum entropy possible in a system where *n* states operate. The *R* (post) was then plotted against *R* (pre) for each lithology and the styles of cyclicity and the way in which cycles are truncated were then interpreted. This concept allows comparisons between states in different system, regardless of the number of state variables selected in each system.

As a measure of depositional environment [41] calculated entropy for the whole sedimentation process
[E (system)] by the following equation:

$$E\,(system) = -\sum_{i=1}^{n}\sum_{j=1}^{n} tij \log_2 tij$$ ..... (eq.**6**)where **tij**$= \frac{Fij}{T}$.

n = the rank of the matrix i.e. the number of rows or columns (five in the present case).

The entropy of the system was then used to decipher the overall depositional environment of cyclical units. The *E*(system) can take a value between $-\log_2 1/n$ **and** $-\log_2 1/n(n-1)$. Data for the tally count matrix at major age unit and at the entire area level were used to compute separately ***E*(pre), *E*(post) and *E*(system)** following the procedure outlined above.

3.3. Stationarity of cyclic sequence

It is always assumed in the analysis of Markov chain, that Markov matrices are the result of a process that is stationary in time and space. According to [53], the term 'stationary' implies that the transition probabilities are constant through time or space. In the present study,stationarity in a sequence was verified by using following chi-square statistics after [54]which has been modified by [53] as:

$$X^2 = 2\sum_{t}^{T}\sum_{ij}^{n} fij(t)\,.\log_e pij(t)/qij$$ ..... (eq.**7**)

where $T = 1, 2, 3, \ldots, T$, giving the number of sequences tested against each other, ***fij*(*t*)** and ***pij*(*t*)** are the tally count and transition probability matrix values, respectively, for each sequence and *qij*equals to the bulk transition probability matrix values calculated for data from both sequences. The number of degrees of freedom equals to $(T-1)n(n-1)$, where *n* equals to total number of lithologic states (5, in the present case). Stationarity of the Markov process is tested at major age level on grouping the entire borehole logs in each major age.

IV. .QUANTITATIVE RESULTS

4.1 Lithologic transition at Major age level

The bulk transition count matrices (*fij*), upward transition probability matrix (P*ij*), downward transition probability Matrix (Q*ij*), independent trial matrix (R*ij*), normalized difference Matrix (D*ij*), expected frequency matrix (E*ij*)and chi-square matrices separately for three major age unitare listed in tables 2, 3 and 4. Data for deducing Markov property in individual major age interval are lumped together and processed at the entire area level for the KNA (Table 3). For each transition pair, the row letter represents the upper facies and the column letter, the lower facies.The facies relationship diagram is presented in figure 3, it has been constructed from the difference matrix (tables 2e, 3e, 4e and 5e).

Table 2aTransitional count matrix (*fij*) for lower Cretaceous Formation, KNA

State	***A***	***B***	***C***	***D***	***E***	***SR***
A	*00*	*33*	*59*	*07*	*02*	***101***
B	*22*	*00*	*30*	*00*	*01*	***53***
C	*75*	*18*	*00*	*09*	*09*	***111***
D	*05*	*01*	*09*	*00*	*00*	***15***
E	*00*	*02*	*11*	*00*	*00*	***13***
SC	***102***	***54***	***109***	***16***	***12***	***293***

Table 2b Upward Transition Probability Matrix(P) for lower Cretaceous Formation, KNA

State	*A*	*B*	*C*	*D*	*E*
A	*0.00*	*0.33*	*0.58*	*0.07*	*0.02*
B	*0.42*	*0.00*	*0.57*	*0.00*	*0.01*
C	*0.68*	*0.16*	*0.00*	*0.08*	*0.08*
D	*0.33*	*0.07*	*0.60*	*0.00*	*0.00*
E	*0.00*	*0.15*	*0.85*	*0.00*	*0.00*

Table 2c Downward Transition Probability Matrix (Q) for lower Cretaceous Formation, KNA

State	*A*	*B*	*C*	*D*	*E*
A	*0.00*	*0.61*	*0.54*	*0.44*	*0.16*
B	*0.23*	*0.00*	*0.28*	*0.00*	*0.08*
C	*0.74*	*0.33*	*0.00*	*0.56*	*0.75*
D	*0.05*	*0.02*	*0.08*	*0.00*	*0.00*
E	*0.00*	*0.04*	*0.10*	*0.00*	*0.00*

Table 2d Independent Trial Matrix(R) for lower Cretaceous Formation, KNA

State	*A*	*B*	*C*	*D*	*E*
A	*0.00*	*0.28*	*0.57*	*0.08*	*0.06*
B	*0.43*	*0.00*	*0.46*	*0.07*	*0.05*
C	*0.55*	*0.29*	*0.00*	*0.09*	*0.07*
D	*0.37*	*0.19*	*0.39*	*0.00*	*0.04*
E	*0.36*	*0.19*	*0.39*	*0.06*	*0.00*

Table 2e Difference Matrix(D) for lower Cretaceous Formation, KNA

State	*A*	*B*	*C*	*D*	*E*
A	*0.00*	*0.05*	*0.01*	*-0.01*	*-0.04*
B	*-0.01*	*0.00*	*0.11*	*-0.07*	*-0.03*
C	*0.13*	*-0.13*	*0.00*	*-0.01*	*0.01*
D	*-0.04*	*-0.12*	*0.21*	*0.00*	*-0.04*
E	*-0.36*	*-0.04*	*0.46*	*-0.06*	*0.00*

Table 2f Expected frequency Matrix(E) for lower Cretaceous Formation, KNA

State	*A*	*B*	*C*	*D*	*E*
A	*00.00*	*28.28*	*57.57*	*08.08*	*06.06*
B	*22.79*	*00.00*	*24.38*	*03.71*	*02.65*
C	*61.05*	*32.19*	*00.00*	*09.99*	*07.77*
D	*05.55*	*02.85*	*05.85*	*00.00*	*00.60*
E	*04.68*	*02.47*	*05.07*	*00.78*	*00.00*

Table 2g chi-square Matrix (X^2) for lower Cretaceous Formation, KNA

State	*A*	*B*	*C*	*D*	*E*
A	*0.000*	*0.787*	*0.036*	*0.144*	*2.720*
B	*0.027*	*0.000*	*1.296*	*3.710*	*1.027*
C	*3.188*	*6.255*	*0.000*	*0.098*	*0.195*
D	*0.055*	*1.200*	*1.696*	*0.000*	*0.600*
E	*4.680*	*0.089*	*6.936*	*0.780*	*00.00*

X^2= 35.52
Degree of freedom= 11,
Limiting value of X^2 at 95% = 19.68

Table 3a. Transitional count matrix (*fij*) for upper Cretaceous Formation, KNA

State	***A***	***B***	***C***	***D***	***E***	***SR***
A	*00*	*44*	*64*	*01*	*15*	***124***
B	*42*	*00*	*25*	*01*	*02*	***70***
C	*66*	*13*	*00*	*06*	*05*	***90***
D	*03*	*02*	*03*	*00*	*00*	***08***
E	*14*	*01*	*05*	*00*	*00*	***20***
SC	***125***	***60***	***97***	***08***	***22***	***312***

Table 3b Upward Transition Probability Matrix (P) for upper Cretaceous Formation, KNA

State	*A*	*B*	*C*	*D*	*E*
A	*0.00*	*0.35*	*0.52*	*0.01*	*0.12*
B	*0.60*	*0.00*	*0.36*	*0.01*	*0.02*
C	*0.73*	*0.14*	*0.00*	*0.07*	*0.00*
D	*0.37*	*0.25*	*0.37*	*0.00*	*0.00*
E	*0.70*	*0.05*	*0.25*	*0.00*	*0.00*

Table 3c Downward Transition Probability Matrix (Q) for upper Cretaceous Formation, KNA

State	*A*	*B*	*C*	*D*	*E*
A	*0.00*	*0.73*	*0.66*	*0.13*	*0.68*
B	*0.34*	*0.00*	*0.26*	*0.13*	*0.09*
C	*0.53*	*0.22*	*0.00*	*0.75*	*0.22*
D	*0.02*	*0.03*	*0.03*	*0.00*	*0.00*
E	*0.11*	*0.02*	*0.05*	*0.00*	*0.00*

Table 3d Independent Trial Matrix (R) for upper Cretaceous Formation, KNA

State	***A***	***B***	***C***	***D***	***E***
A	*0.00*	*0.32*	*0.52*	*0.04*	*0.12*
B	*0.50*	*0.00*	*0.38*	*0.03*	*0.09*
C	*0.58*	*0.28*	*0.00*	*0.04*	*0.10*
D	*0.41*	*0.20*	*0.32*	*0.00*	*0.07*
E	*0.43*	*0.20*	*0.33*	*0.03*	*0.00*

Table 3e Difference Matrix (D) for upper Cretaceous Formation, KNA

State	***A***	***B***	***C***	***D***	***E***
A	*0.00*	*0.03*	*0.00*	*-0.03*	*0.00*
B	*0.10*	*0.00*	*-0.02*	*-0.02*	*0.07*
C	*0.15*	*-0.14*	*0.00*	*0.03*	*-0.01*
D	*-0.04*	*0.05*	*0.05*	*0.00*	*-0.07*
E	*0.27*	*-0.15*	*-0.08*	*-0.03*	*0.00*

Table 3f Expected frequency Matrix (E) for upper Cretaceous Formation, KNA

State	***A***	***B***	***C***	***D***	***E***
A	*00.00*	*39.68*	*64.48*	*04.96*	*14.88*
B	*35.00*	*00.00*	*26.60*	*02.10*	*06.30*
C	*52.20*	*25.20*	*00.00*	*03.60*	*09.00*
D	*03.28*	*01.60*	*02.56*	*00.00*	*00.56*
E	*08.60*	*04.00*	*06.60*	*00.60*	*0.00*

Table 3g chi-square Matrix (X^2) for upper Cretaceous Formation, KNA

State	*A*	*B*	*C*	*D*	*E*
A	*0.000*	*0.470*	*0.004*	*3.160*	*0.001*
B	*1.400*	*0.000*	*0.096*	*0.576*	*2.935*
C	*3.648*	*5.906*	*0.000*	*1.600*	*1.778*
D	*0.024*	*0.100*	*0.076*	*0.000*	*0.560*
E	*3.390*	*2.250*	*0.388*	*0.600*	*0.000*

X^2= 20.32
Degree of freedom= 11,
Limiting value of X^2 at 95% = 19.68

Table 4a Transitional count matrix (*fij*) for Tertiary Formation, KNA

State	*A*	*B*	*C*	*D*	*E*	*SR*
A	*00*	*09*	*101*	*03*	*02*	***115***
B	*11*	*00*	*09*	*00*	*00*	***20***
C	*98*	*10*	*00*	*06*	*03*	***117***
D	*03*	*00*	*05*	*00*	*02*	***10***
E	*05*	*00*	*01*	*01*	*00*	***07***
SC	***117***	***19***	***116***	***10***	***07***	***269***

Table 4b Upward Transition Probability Matrix(P) for Tertiary Formation, KNA

State	*A*	*B*	*C*	*D*	*E*
A	*0.00*	*0.08*	*0. 88*	*0.03*	*0.02*
B	*0.55*	*0.00*	*0.45*	*0.00*	*0.00*
C	*0.84*	*0.09*	*0.00*	*0.05*	*0.03*
D	*0.30*	*0.00*	*0.50*	*0.00*	*0.20*
E	*0.71*	*0.00*	*0.14*	*0.14*	*0.00*

Table 4c Downward Transition Probability Matrix (Q) for Tertiary Formation, KNA

State	*A*	*B*	*C*	*D*	*E*
A	*0.00*	*0.47*	*0.87*	*0.30*	*0.29*
B	*0.09*	*0.00*	*0.08*	*0.00*	*0.00*
C	*0.84*	*0.53*	*0.00*	*0.60*	*0.43*
D	*0.03*	*0.00*	*0.04*	*0.00*	*0.28*
E	*0.04*	*0.00*	*0.01*	*0.10*	*0.00*

Table 4d Independent Trial Matrix (R) for Tertiary Formation, KNA

State	*A*	*B*	*C*	*D*	*E*
A	*0.00*	*0.13*	*0.76*	*0.07*	*0.03*
B	*0.47*	*0.00*	*0.46*	*0.04*	*0.03*
C	*0.76*	*0.12*	*0.00*	*0.07*	*0.05*
D	*0.45*	*0.07*	*0.45*	*0.00*	*0.03*
E	*0.45*	*0.07*	*0.44*	*0.04*	*0.00*

Table 4e Difference Matrix (D) for Tertiary Formation, KNA

State	*A*	*B*	*C*	*D*	*E*
A	*0.00*	*-0.05*	*0.12*	*-0.04*	*-0.01*
B	*0.08*	*0.00*	*-0.01*	*0.00*	*-0.03*
C	*0.08*	*-0.03*	*0.00*	*-0.02*	*-0.02*
D	*-0.15*	*0.00*	*0.05*	*0.00*	*-0.01*
E	*0.26*	*0.00*	*-0.3*	*0.10*	*0.00*

Table 4f Expected frequency Matrix(E) for Tertiary Formation, KNA

State	*A*	*B*	*C*	*D*	*E*
A	*0.00*	*14.95*	*87.4*	*8.05*	*3.45*
B	*9.40*	*0.00*	*9.20*	*0. 80*	*0.60*
C	*88.9*	*14.04*	*0.00*	*8.19*	*5.85*
D	*4.50*	*0.70*	*4.50*	*0.00*	*0.30*
E	*3.15*	*0.49*	*3.08*	*0.28*	*0.00*

Table 4g chi-square Matrix (X^2) for Tertiary Formation, KNA

State	*A*	*B*	*C*	*D*	*E*
A	*0.000*	*2.368*	*2.116*	*3.168*	*0.609*
B	*0.272*	*0.000*	*0.004*	*0.800*	*0.600*
C	*0.930*	*1.163*	*0.000*	*0.586*	*1.388*
D	*0.500*	*0.700*	*0.056*	*0.000*	*9.633*
E	*1.087*	*0.490*	*1.400*	*1.850*	*0.000*

X^2= 29.72
Degree of freedom= 11,
Limiting value of X^2 at 95% = 19.68

Table 5a Transitional count matrix (*fij*) for entire study area (KNA)

State	*A*	*B*	*C*	*D*	*E*	***SR***
A	*00*	*86*	*224*	*11*	*19*	***340***
B	*75*	*00*	*64*	*01*	*03*	***143***
C	*239*	*41*	*00*	*21*	*17*	***318***
D	*11*	*03*	*17*	*00*	*02*	***33***
E	*19*	*03*	*17*	*01*	*00*	***40***
SC	***344***	***133***	***322***	***34***	***41***	***874***

Table 5b Upward Transition Probability Matrix(P) for entire study area (KNA)

State	*A*	*B*	*C*	*D*	*E*
A	*0.00*	*0.25*	*0. 66*	*0.03*	*0.06*
B	*0.52*	*0.00*	*0.45*	*0.01*	*0.02*
C	*0.75*	*0.13*	*0.00*	*0.07*	*0.05*
D	*0.33*	*0.09*	*0.05*	*0.00*	*0.06*
E	*0.48*	*0. 08*	*0.43*	*0.03*	*0.00*

Table 5c Downward Transition Probability Matrix(Q) for entire study area (KNA)

State	*A*	*B*	*C*	*D*	*E*
A	*0.00*	*0.65*	*0.70*	*0.32*	*0.46*
B	*0.22*	*0.00*	*0.20*	*0.03*	*0.07*
C	*0.69*	*0.31*	*0.00*	*0.62*	*0.41*
D	*0.03*	*0.02*	*0.05*	*0.00*	*0.05*
E	*0.06*	*0.02*	*0.05*	*0.03*	*0.00*

Table 5d Independent Trial Matrix(R) for entire study area (KNA)

State	*A*	*B*	*C*	*D*	*E*
A	*0.00*	*0.25*	*0.61*	*0.06*	*0.07*
B	*0.46*	*0.00*	*0.43*	*0.05*	*0.06*
C	*0.62*	*0.24*	*0.00*	*0.06*	*0.07*
D	*0.41*	*0.16*	*0.38*	*0.00*	*0.05*
E	*0.41*	*0.16*	*0.38*	*0.04*	*0.00*

Table 5e Difference Matrix (D) for entire study area (KNA)

State	*A*	*B*	*C*	*D*	*E*
A	*0.00*	*0.00*	*0.05*	*-0.03*	*-0.01*
B	*0.06*	*0.00*	*0.02*	*-0.04*	*-0.04*
C	*0.13*	*-0.11*	*0.00*	*0.01*	*-0.02*
D	*-0.08*	*-0.07*	*-0.33*	*0.00*	*0.01*
E	*0.07*	*-0.09*	*0.05*	*-0.01*	*0.00*

Table 5f Expected frequency Matrix (E) for entire study area (KNA)

State	*A*	*B*	*C*	*D*	*E*
A	*0.00*	*85.0*	*207.4*	*20.4*	*23.8*
B	*65.8*	*0.00*	*61.5*	*07.2*	*08.6*
C	*197.2*	*76.3*	*0.00*	*19.1*	*22.3*
D	*13.5*	*05.3*	*12.5*	*0.00*	*01.7*
E	*16.4*	*06.4*	*15.2*	*01.6*	*0.00*

Table 5g chi-square Matrix (X^2) for entire Formations in the KNA

State	*A*	*B*	*C*	*D*	*E*
A	*0.000*	*0.012*	*1.329*	*4.331*	*0.968*
B	*1.286*	*0.000*	*0.102*	*5.339*	*3.647*
C	*8.860*	*16.33*	*0.000*	*0.189*	*1.259*
D	*0.462*	*0.988*	*1.620*	*0.000*	*0.053*
E	*0.142*	*1.806*	*0213.*	*0.225*	*0.000*

X^2= 49.44
Degree of freedom= 11,
Limiting value of X^2 at 95% = 19.68

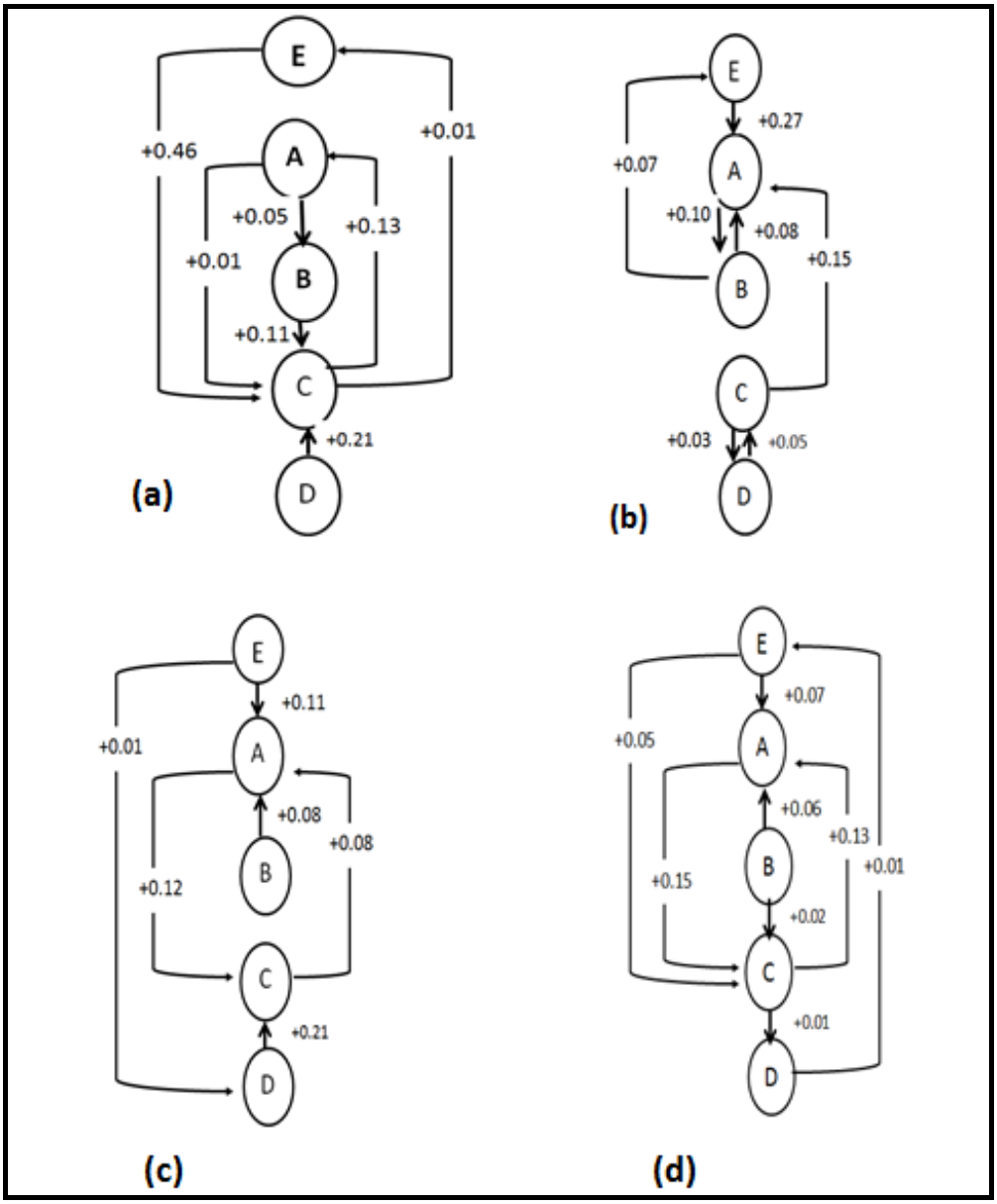

Fig.2:Lithofacies relationship diagram showing downward transitions (based on positive values in *Dij*matrix) in the three age groups (a= lower Cretaceous, b=upper Cretaceous, c= Tertiary) and d for the entire KNA Formations.

4.2 Result of entropy analysis at major age level

The computed entropies *E*(pre) and *E*(post), normalized entropies *R*(pre) and *R*(post) of each lithologic state are presented in Tables 6.The entropy sets for the lithofacies of the area at major age intervals are presented in Fig.3 and the relationship between entropy and depositional environment of lithological sequences is presented on Fig.4

Table 6a. Entropy with respect to deposition of lithologies in the lower Cretaceous Formation

State	$E^{(post)}$	$E^{(pre)}$	$R^{(pre)}$	$R^{(post)}$	*Relationship*
A	*1.368*	*1.865*	*0.933*	*0.684*	$E^{(pre)} > E^{(post)}$
B	*1.058*	*1.298*	*0.649*	*0.529*	$E^{(pre)} > E^{(post)}$
C	*1.390*	*1.634*	*0.817*	*0.695*	$E^{(pre)} > E^{(post)}$
D	*1.242*	*0.623*	*0.312*	*0.621*	$E^{(pre)} < E^{(post)}$
E	*0.612*	*0.519*	*0.260*	*0.306*	$E^{(pre)} < E^{(post)}$
E(max) = 2.0 E(system)= 3.219					

Table 6b. Entropy with respect to deposition of lithologies in the upper Cretaceous Formation

State	$E^{(post)}$	$E^{(pre)}$	$R^{(pre)}$	$R^{(post)}$	*Relationship*
A	*1.456*	*1.494*	*0.747*	*0.728*	$E^{(pre)} > E^{(post)}$
B	*1.155*	*1.735*	*0.868*	*0.578*	$E^{(pre)} > E^{(post)}$
C	*1.000*	*1.825*	*0.913*	*0.500*	$E^{(pre)} > E^{(post)}$
D	*1.568*	*0.417*	*0.209*	*0.784*	$E^{(pre)} < E^{(post)}$
E	*1.080*	*0.681*	*0.341*	*0.540*	$E^{(pre)} < E^{(post)}$
	E (max) = 2.0 E(system)= 3.226				

Table 6c. Entropy with respect to deposition of lithologies in the Tertiary Formation

State	$E^{(post)}$	$E^{(pre)}$	$R^{(pre)}$	$R^{(post)}$	*Relationship*
A	*0.721*	*1.731*	*0.866*	*0.361*	$E^{(pre)} > E^{(post)}$
B	*0.996*	*0.477*	*0.239*	*0.498*	$E^{(pre)} < E^{(post)}$
C	*0.894*	*1.668*	*0. 834*	*0.447*	$E^{(pre)} > E^{(post)}$
D	*1.137*	*0. 854*	*0.427*	*0.569*	$E^{(pre)} < E^{(post)}$
E	*1.148*	*0.585*	*0.293*	*0.574*	$E^{(pre)} < E^{(post)}$
E(max) = 2.0 E(system)= 2.477					

Table 6d. Entropy with respect to deposition of lithologies in the entire KNA Formations

State	$E^{(post)}$	$E^{(pre)}$	$R^{(pre)}$	$R^{(post)}$	*Relationship*
A	*1.295*	*1. 810*	*0.905*	*0.648*	$E^{(pre)} > E^{(post)}$
B	*1.191*	*1.369*	*0.685*	*0.596*	$E^{(pre)} > E^{(post)}$
C	*1.181*	*1. 855*	*0.928*	*0.591*	$E^{(pre)} > E^{(post)}$
D	*1.304*	*0.699*	*0.350*	*0.652*	$E^{(pre)} < E^{(post)}$
E	*1.480*	*0.574*	*0.287*	*0.740*	$E^{(pre)} < E^{(post)}$
	E(max) = 2.0 E(system)= 3.093				

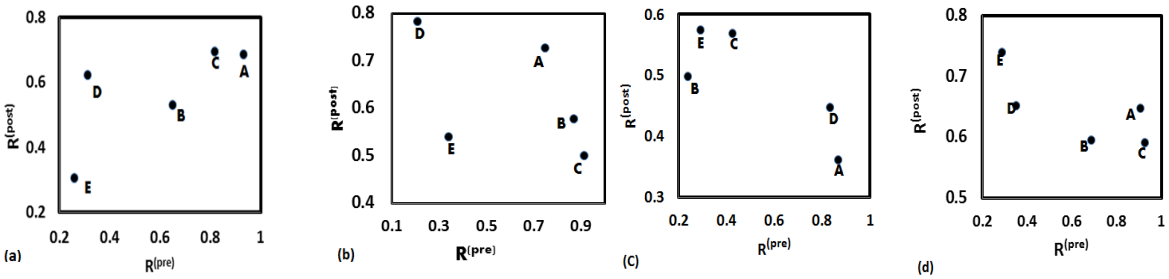

Fig.3. Entropy sets for the lithofacies of the KNA Formations in three major age intervals a)lower Cretaceous, b)upper Cretaceous, c) Tertiary and d)the entire area. A: Shale, B: Interbedded sandstone-shale, C: Coarse to medium grained sandstone, D: Conglomerate, and E: Carbonate and argillaceous shale.

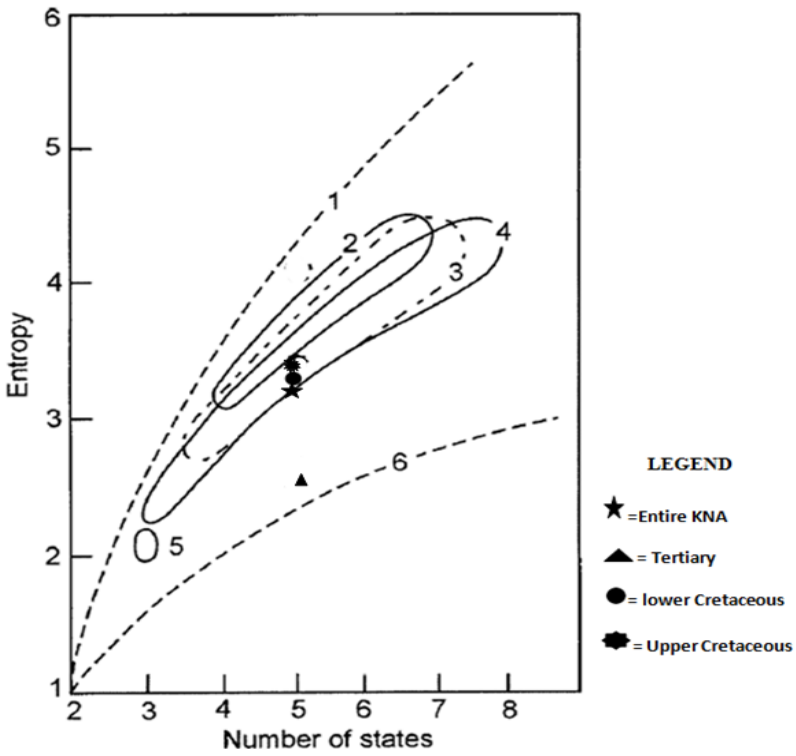

Fig .4: Relationship between entropy and depositional environment of lithological sequences (modified *after* Hattori, 1976). **1**: Maximum entropy, **2**: Entropies for the coal-measure successions, **3**: Entropies for fluvial-alluvial successions, **4**: Entropies for neritic successions, **5**: Entropies for flysch sediments, **6**: Minimun entropy,

4.3. Result of Chi-square stationarity of cycle's sequence

The result of the Chi-square stationarity of cycles within formations of the KNA is presented in Table 7.

Table 7.Chi-square stationarity statistics within formations of the KNA.

Major age interval	X^2	*Limiting values*		*Markov process*
		99%	*95%*	
LC-UC	*29.37*	*37.57*	*31.41*	*Stationary*
LC-T	*17.15*	*37.57*	*31.41*	*Stationary*
UC-T	*20.68*	*37.57*	*31.41*	*Stationary*

LC= lower Cretaceous, UC=upper Cretaceous, T=Tertiary

V. Interpretations and Discussion

5.1 Markov Chain Analyses

Randomness test was performed by Markovian property using standard chi–square test. The chi–square statistics for the KNA succession using five rock types reveal that the test has been passed by all three age groups and the entire study area at an appropriate degree of freedom at 95% level of confidence. The facies relationship diagram (Fig.2d) for the entire study area suggests that the KNA cycles are coarsening-downward (fining upward) asymmetric type. Each complete cycle starts with carbonate and argillaceous shale (facies E) at the top and is been followed by dark/grey shale (facies A) and sandstone facies (facies B and C) and the cycles is been terminated by the conglomerate facies (facies D) at the base. Predominance of truncated coarsening-downward cycles with abrupt changes in lithology at the top, suggests deposition of KNA sediment by rapidly shifting braided streams. Had the deposition in meandering stream depositional environment as in the case of Barakar and Barren Measures Formations [44], then the cycles would have been gradually fining upward sequence.

The excess of probability of transition of A to C and C to A over random transition are 0.05 and 0.13 respectively (Fig.2d), which indicate frequent braiding of the stream channels that lead to the superposition and inter-fingering of proximal channel facies (C) by proximal flood plain, abandoned channel fill and over bank facies (A) and vice versa. The excess of probability of bar-top and abandoned-channel deposits (facies B) overlying distal-channel bars deposit facies (C) is 0.02, which suggest that

the channels were more frequently abandoned, a feature generally common in braided streams than sidewise migration of meandering stream and deposition of fine-grained sandstones[2]. This indicates dominance of braided stream regime during sedimentation in KNA. The inter bedded fine-grained sandstones and shale (facies B) have strong tendency to be succeeded by dark/grey shale (facies A) than coarse to medium grained sandstone facies (facies C) with difference probability of 0.06 and 0.02 respectively. These features suggest that many of the abandoned channels received fine clastics during the periods of greater discharge while a few of them were deposited at the distal-channel bars. The distal-channel bars deposit is the dominant lithofacies, which shares about 36% by volume of the KNA Formation by volume. The probability that this distal-channel bars deposit can be followed by the shale dark/grey shale (A) is 0.13 which is higher than it been converted to conglomerate. Therefore, the depositional process in the area continued in a non- random situation but may not always possess well-defined cyclic patterns.

5.2 Entropy model for the KNA Succession

Comparison ofE(pre)with E(post) for each facies state shows that the memory of each facies state for either the successor state or the precursor state is non – random but non – cyclic . It is also observed that there is no cases where$E(pre) \approx E(post) \neq 0.0$ which indicates some level of dependency of one state on the other. When the lithologic states are examined in terms of the relationships between E(pre) and E(post) values , it is found that E(pre) values are higher than E(post) value in most of the sequences (especially within the various age groups) and in few others E(post) values are greater than E(pre) values. The former relationship (E(pre)> E(post)) in mathematical terms indicates that the dependency of one lithologic state on its precursor is not even and it can possibly occur after different state. In the later (E(post)> E(pre)) situation ,the dependency of one lithologic state on its precursor is stronger than its influence on the successor.

For the lithological states A, B, C for lower Cretaceous sediments (Table 6a), E(pre) >E(post) indicating that deposition of these lithologies (shale facies, inter-bedded fine-grained sandstone facies and coarse to medium-grained sandstone) did not depend largely on the lithological composition of the underlying strata but exerted a considerable influence upon succeeding lithological states. In other words, lithologies that follow dark/grey shale facies, inter-bedded fine-grained sandstone facies and coarse to medium-grained sandstone facies can be conjectured with more certainty than those preceding themfollowing [41] interpretation. E(pre) < E(post) relationship in cases of conglomerateand carbonate and argillaceous shale facies suggest that these facies do not show strong memory for any succeeding lithological state but are dependent on the preceding state in the succession.

For the upper Cretaceous sediments, the E(pre) >E(post) for facies A, B, C which implies that there is a high probability of these states passing up into another state. By contrast, the cases of carbonate and argillaceous shale and conglomeratefacies$E$(post) > E(pre) suggest that these facies do not show strong memory for any succeeding lithological state but are dependent on the preceding state in the succession.

For Tertiary sediments, the E(pre) >E(post) for facies A and C which implies a high probability of these states passing up into another state A → C or vice versa. Facies relationship diagram (Fig.2c) supports this view. For the lithological states B, D and E the E(post) > E(pre), which implies that there is a lower probability of these state passing up to another state and that the deposition of these lithofacies are strongly influenced by the preceding state in the succession.

The variations in pre- and post-depositional entropy values suggest variable degree of dependency of lithofacies on precursor and influence on successor during sedimentation in the entire KNA. E(pre) > E(post) relationship (Table 6d.) in case of dark/grey shale and interbedded fine grained sandstone and shale and coarse to medium-grained sandstonefacies indicates that the dependency of these lithologic state on their precursors in the entire study area is not even and it can occur after different state. In other words the deposition of dark/grey shale and inter-bedded fine grained sandstone and shale facies, did not depend largely on the lithologic composition of the underlying strata but exerted a considerable influences upon succeeding lithostrata. By contrast, for the lithological states D and E (which shares less than 9% by volume of the KNA Formation by volume) the E(post) > E(pre), an indication that these states were deposited in specific depositional conditions but used to overlain by a wide variety of different strata[41].

These relationships support in a statistical way the otherwise geologically obvious conclusion that the deposition of these lithologies in the DKC basin depends largely on specific environments[18]. At all level Carbonate and argillaceous shale and conglomerate are having E(post) > E(pre) which means that the occurrence of thesefacies within the sequence at all major age level depend on the preceding state in the succession.

The plot of the R (pre) and R(post) values for each lithological state is given in the figure 3 of Hattori's diagrams. The R(pre)-R(post) plots of the facies states (Fig. 3) resemble closely with those for sediment which [41] assigned to be the A-4 type. The lithological cycles in the KNA are dominantly asymmetric cycles.

The lower Cretaceous Formations which are the oldest sedimentary units in the area is having theE(System) value of 3.219. The upper Cretaceous Formations are havingthe highest E(system) value of 3.226 for the study area. The Tertiary Formations are having the lowest E(System) value (2.477).This implies that the highest degree of randomness of the KNA sedimentation system was during the Cretaceous.According [23], passive margin wedge was deposited during this period (Cretaceous) and was marked by a short compressive episode localized along the transfer faults which are present in the eastern part of the DSB. The Albian–Coniacian time in the DKC basin was characterized by rotational fault blocks, gravity sliding and salt movement [18 and 27]. These structures are linked to the gravitational instability of the margin and can explain for the highest rate of randomness in the deposition of sediments as seen in the present study. However the late gravity sliding caused by uplift in the Tertiary [18] resulted in lower rate of randomness in the deposition of sediments than those of the Cretaceous time.

When the E(system) values for KNA sedimentation sequences are evaluated in terms of broad depositional environment by plotting E (system) against the number of states

(Fig.4) , most of the points (lower Cretaceous, Upper Cretaceous and the entire study area) occur within the fields of (3) corresponding to the'fluvial-alluvial system' (Fig. 4) delineated by [41]. However the entropy of the Tertiary sedimentation system as shown in Fig.4the points lie in the undefined envelope between the neritic field and the line of minimum possible entropy in the succession discrimination diagram of [41]. The *E*(System) for the Tertiary succession are low(2.477) indicating lower degree of randomness of the Tertiary sedimentation system.

5.3 Stationarity of cyclic sequence

The highest calculated value of chi-square statistics is 29.37 (Table 7), which at 20 degrees of freedom is below the limiting value of 31.41 at 95% significance level; emphasizing that at each major age level the sequence of lithologic transitions has been stationary through space. The results suggest that the nature of the cyclic sequence is stationary at major age level and strongly indicates that the corresponding set of sub-environments in the depositional basin conformsto a definite pattern.

VI. SUMMARY AND CONCLUSION

The lithologies in the KNA have been conveniently grouped under five facies states viz. (A) dark grey shale-, (B) inter-bedded fine grained sandstone and shale -, (C) Coarse to medium-grained sandstone-, (D) Conglomerate faciesand (E) Carbonate and argillaceous shale for statistical analyses. The application of improved Markov process model and entropy functions evidently indicate asymmetrical cyclic pattern for sediments of the KNA.The sequenceexhibits upward decrease of grain size, which is possibly due to decline of flow intensity and current velocity coupled with lateral migration of streams during deposition of each cycle. The lithofacies constituting the fining-upward cycles can be linked with different subenvironments of braided channel fluvial system and their organization may be ascribed to lateral migration of streams in response to differential subsidence.

Each complete fining upward cycle start with medium to fine -grained sandstone (facies C) or coarse grained sandstone and conglomerate (facies D)and terminating with shale (dark/grey and carbonate and argillaceous shale) suggesting the establishment of some kind of channel system and subsequently its abandonment by stream and entombment beneath freshly deposited coarse clastics. The coarse to medium –grained sandstone facies shares about 36% of the KNA Formations by volume. The sandstone facies is probable alluvianfacies. The interbedded fine-grained sandstone/shale (faciesB) and shale (facies A), preferentially overlie coarse to medium-grained sandstone throughout the study area. These lithofacies respectively constitutes about 16% and 39% of the given KNA area sequence. The interbedded assemblages of the fine clastics is attributed to deposition by vertical/lateral accretion on top of channel bars during a low water stage or as overbank/levee facies during periods of overflow. Following the flood stage, laccustrine conditions of stagnant water may have developedin the low lying areas beyond channel and overbank sub-environments, resulting in the deposition of shale/carbonaceous shale forming sub environments where swamp or marshy conditions develop.

Indeed, interbedded fine-grained sandstone/shale (facies B) records a strong upward transition to shale (*Zij*= +0.13). However, upward linkage of shale (facies A), which represents the top unit of KNA fining cyclical units has more preference for coarse to medium-grained sandstone (facies C) than interbedded fine-grained sandstone/shale (facies B) resulting in the asymmetrical cycles. This implies a gradual encroachment of shale swamp by adjacent back swamp and levee sub-environments as a consequence of slow and gradual lateral shift of channel course across the alluvial plain of meandering streams.

The KNA cycles belong to the D-type cyclic sequences of [41] which are essentially random lithologic series as evidenced by entropy analysis. The deposition of sandstones {E(pre) of 1. 855 } represents the most random event, which was possibly brought about by unsystematic change in the depositional mechanism triggered by differential subsidence of the depositional area. Intra-basinal differential subsidence might have been responsible for the rejuvenation and lateral migration of the river system and consequent initiation of a new cycle with freshly transported sediments.

VII. CONCLUSION

The present study is designed to quantify the nature of cyclicity observed within the Formationsin the KNA onshore DKC basin using modified Markov chain analysis and entropy functions. The cyclical sequence shows fining upward characters and is commonly asymmetrical represented by coarse to medium-grained sandstone → interbedded finesandstone and shale → shale, similar to Hattori's type 'D' pattern. This order of lithologic transition for the Cretaceous section is closely comparable with that suggested for the lower Cretaceous Formations measures of DKC basin [14 and 15]. The Markov chain and entropy pattern substantiated proposed fluvial-alluvia depositional model for the sub basin as derived independently from outcrop analysis [15]. The deposition of conglomerate and carbonaceous shale represents the random event, which was possibly brought about by unsystematic change in the depositional mechanism triggered by differential subsidence of the depositional area. Intra-basinal differential subsidence might have been responsible for the rejuvenation and lateral migration of the river system and consequent initiation of a new cycle with freshly transported sediments. Rapid and frequent lateral shift of channel course, a common phenomenon in modern river basin may favourably explain the development of asymmetrical fining upward cycles. However, those cycles which enclose thick shale beds exhibiting sharp relationship between lithofacies possibly developed due to the differential subsidence of the depositional basin.

ACKNOWLEDGEMENT

The borehole record and well log data set for thisstudywasprovided by the National Hydrocarbon Corporation

(Cameroon) through the cooperationwith the University of Buea and the authorisdeeplygrateful.

REFERENCES

[1] Abolo, M.G.C. (1996). Evaluation du Potentiel en Hydrocarbures dans Les Series Du Cretace De La Region De Kribi-Campo (Basin de Douala/Kribi-Campo). SNH. p121

[2] Miall, A. D. (1985). Architectural-elementanalysis: A new method of facies analysisapplied to fluvial deposits. Earth Science Reviews, 22:261-308.

[3] Selly, R. (1978). Ancient Sedimentary Environment 2nd ed., Chapman and Hall, London.

[4] Walker, R. G. (1984). General Introduction. In: Faciesmodels, 2nd edn. Geological Society. Canada Reprint Series 1, 1-10.

[5] Hota R. N. and Maejima W. (2004). Comparative study of cyclicity of lithofacies in Lower Gondwana formations of Talchir basin, Orissa, India: A statisticalanalysis of sub-surface logs; Gondwana Res. 7 353–362.

[6] Walther J. (1893). Einleitung in de GeologiealshistorischeWissenschaft-Jena; V. 1055

[7] Reading H. G. (1991). SedimentaryEnvironments and Facies; 2ndedn. (London: Blackwell) 641p

[8] Sengupta, S. M. (2006). Introduction to Sedimentology; 2ndedn. (New Delhi: Oxford and IBH Publishing Co.) 314pp.

[9] Tewari, R. C, Singh, D. P. and Khan, A. Z. (2009). Application of Markov chain and entropyanalysis to lithologic succession – an examplefrom the earlyPermianBarakar Formation, Bellampallicoalfield,AndhraPradesh, India J. EarthSyst. Sci. 118, No. 5, October 2009, pp. 583–596

[10] Maria, B.S, Durán EL, Aldana M. (2014).StratigraphicColumnsModeling and CyclicityAnalysis of the Misoa Formation, Maracaibo Lake, Venezuela, using Markov Chains. GeofísicaInternacional 53: 277-288.

[11] Schwarzacher, W. (1969). The use of Markov chains in the study of sedimentary cycles. Jour Math Geol 1: 17-39.

[12] Regnout, J.M. (1986) Synthèse géologique du Cameroun. D.M.G., Yaoundé, Cameroun, p118.

[13] Nguene, F.R., Tamfu, S., Loule, J.P.andNgassa, C.(1992). Paleoenvironments of the Douala and Kribi-Campo Sub Basin in Cameroon, West Africa.Geologie Africaine: Coll.Geol.Libreville, Recueil des Communic, 129-139

[14] ECL (Exploration Consultant Limited) (2001): An Integrated Study Of Structural Development, Source Rock Maturity And Hydrocarbon Generation In the Douala/Kribi-Campo Basin. SNH internal report, Non-Exclusive Report

[15] Ntamak-Nida,, M.J., Baudin, F., Schnyder, J., Makong, J.-C., Mpesse. J. E, Komguem, P.B., Abolo, G.M (2010). Sedimentology and sequencestratigraphyfromoutcrops of the Kribi-Campo sub-basin: LowerMundeck Formation (LowerCretaceous, southernCameroon). Journal of AfricanEarth Sciences 58 1–18

[16] Burker, K. and Whiteman, A.J. (1972). Uplift, rifting and break-up of Africa: studies in Earth and spaces, Geol. Soc. Amer. Memoir 132. 738-755

[17] Lawrence, S.R., Munday, S., Bray, R.. (2002). Regionalgeology and geophysics of the eastern Gulf of Guinea (Niger Delta to Rio Muni). The LeadingEdge 1113-1117.

[18] Loule, J.P.andNgassa, C. (1992): Paleoenvironments of the Douala and Kribi-Campo Sub Basin in Cameroon, West Africa. Geologie Africaine: Coll.Geol.Libreville, Recueil des Communic, 129-139.

[19] Batupe, M., Abolo, M.G., (1997). Guide book field trip No. 2. Mesozoicsyn-rift deposits of the Campo region in the Douala/Kribi-Campo basin. In: 13th Colloquium of AfricanMicropaleontology. 3rd Colloquium on the Stratigraphy and Paleontology of the South Atlantic. 2nd Annual Meeting of the IGCP Project No. 381.

[20] Pauken, R.J., (1992). Sanaga Sud field, offshore Cameroon, West Africa. In: Halbouty, M.T. (Ed.), GiantOil and Gas Fields of the Decade 1978–1988, vol. 54. American Association of PetroleumGeologistsMemoir, pp. 217–230.

[21] Reyre, D., (1966). Histoire géologique du bassin de Douala. In: Reyre, D. (Ed.), Symposium sur les bassins sédimentaires du littoral africain. Association du Service Géologique d'Afrique, IUGS, pp. 143–161.

[22] Benkhelil, J., Giresse, P., Poumot, C., Ngueutchoua, G., (2002).Lithostratigraphic, geophysical and morpho-tectonicstudies of the South Cameroonshelf. Mar. Petr. Geol. 19, 499–517.

[23] Meyers, J.B., Rosendahl, B.R., Groschel-Becker, H., Austin, Jr.J.A., Rona, P.A., (1996). Deeppenetrating MCS imaging of the rift-to drift transition, offshore Douala and North Gabon basins, West Africa. Marine and PetroleumGeology 13 (7), 791–835.

[24] Teisserenc, P., Villemin, J., (1989). Sedimentary basin of Gabon-Geology and oilsystems. In: Edwards, J.D., Santogrossi, P.A. (Eds.), Divergent/Passive Margin Basins, vol. 46. American Association of PetroleumGeologistsMemoir, pp. 117–199.

[25] Reyment, R.A., Tait, E.A., (1972). Biostratigraphicaldating of the earlyhistory of the South Atlantic. The Philosophical Transactions of the Royal Society of London,Series B 264, 55–95.

[26] Tissot, B. Demaison, G. Masson, J. R. Delteil and Conbaz, A. (1980). "Paleoenvironment and PetroleumPotential of Middle Creataceous Black Shales in Atlantic Basin," AAPG Bulletin, Vol. 64, 2051-2063

[27] Turner, J. P. (1999). "DetachmentFaulting and PetroleumProspectivity in the Rio Muni Basin, Equatorial Guinea, West Africa," In: N. R. Cameroon, R. H. Bate and V.-S. Clure, Eds., The Oil and Gas Habitats of the South Atlantic, Vol. 153, Geological Society Special Publications, 303-320.

[28] Udden, J. A. (1912). Geology and MineralReso Quadrangle, Illinois, US Geological Survey Bulletin, No. 506, , p. 103

[29] Weller, J. M. (1930) "CyclicalSedimentation of the Pensylva-nianPeriod and ItsSignificance," Journal of Geology, Vol. 38, No. 2, , pp. 97-135

[30] Read W. A. (1969). Analysis and simulation of Namuriansedi-ments in central Scotland using a Markov process model; MathematicalGeol. 1 199–219.

[31] Casshyap, S. M. (1975). Cyclicchara cteristics of coalbearingsediment in the Bochumer Formation (Westphal A-2) Ruhrgebiet, Germany; Sedimentology22, 237–255.

[32] Allen , J.R.L. ,(1965a). Fining upward cycle in alluvial succession. Liverpool, Mqnchester Geol.Jour.,4 229-246

[33] Strahaler, A. N. (1963). The Earth Sciences, Harper and Row, New York, 681,

[34] Miall, A. D. (1973). Markov chainanalysisapplied on an ancient alluvial plain succession, Sedimentology, 20:347-364.

[35] Casshyap, S. M. (1975).Cyclicchara cteristics of coalbearingsediment in the Bochumer Formation (Westphal A-2) Ruhrgebiet, Germany; Sedimentology22 237–255

[36] Cant, D. J and Walker, R. G. (1976). Development of a braided-fluvial facies model for the DevonianBattery Point Sandstone, Quebec, Canadian Journal of Earth Science, 13:102-119

[37] Sengupta, S. M. (2006) Introduction to Sedimentology; 2ndedn. (New Delhi: Oxford and IBH Publishing Co.) 314p .

[38] Vistelius A. B. (1949). On the question of the mechanism of formation of strata; Dokl. Acad. Nauk. SSSR 65 191–194.

[39] Krumbein, W. C. and M. F. Dacey, (1969). Markov chains and embedded Markov chains in Geology. Journal of MathematicalGeology, 1:79-86

[40] Kulatilake, P. H. S. W. (1987). Modeling of cyclicalstratigraphyusing Markov chains. International Journal of Mining and Geological Engineering, 5:121-130.

[41] Hattori, I. (1976). Entropy in Markov chains and discrimination of cyclic patterns in lithologic successions; Math. Geol. 8 477–497.

[42] Khan Z A (1997). Quasi-independence and entropyanalysis of a lateorogenic Middle Siwalik molasses sequence in Kuluchaur area, PauriGarhwal, India; Geoinformatics7 135–145.

[43] Sharma, S. Sharma, M. and Singh, I. B. (2001). Facies charac-teristics and cyclicity in lower Siwalik sediments, Jammu area: A new perspective; Geol. Mag. 138 455–470.

[44] Hota R N and Maejima W. (2004). Comparative study of cyclicity of lithofacies in Lower Gondwana formations of Talchir basin, Orissa, India: A statisticalanalysis of sub-surface logs; Gondwana Res. 7 353–362.

[45] Khan Z. A. and Tewari R. C. (2007). Quantitative model of earlyPermiancoalbearing cycles from Son-Mahanadi and Koel-Damodar

basins of eastern-central India; Gondwana Geol. Magazine, Spec. Publ.9 115–125.

[46] Tewari R. C, Singh D. P. and Khan A. Z. (2009): Application of Markov chain and entropyanalysis to lithologic succession – an examplefrom the earlyPermianBarakar Formation, Bellampallicoalfield,AndhraPradesh, India J. EarthSyst. Sci. 118, No. 5, October 2009, pp. 583–596

[47] Khan Z.A, Tewari R.C (2013).Geo-statisticalanalysis of the Barakarcyclothems (EarlyPermian): A case studyfrom the subsurface logs in Singrauli Gondwana Sub-basin of Central India. Int J GeolEarth Environ Sci 3: 1-22.

[48] Gingerich P D (1969). Markov analysis of cyclical alluvial sedi-ments; J. Sedim. Petrol. 39 330–332.

[49] Power D W and Easterling G R (1982).Improvedmethodology for usingembedded Markov chains to describecyclicalsediments; J. Sedim. Petrol. 53 913–923.

[50] Read W A (1969). Analysis and simulation of Namuriansediments in central Scotland using a Markov process model; MathematicalGeol.1 199–219

[51] Pelto C.R.(1954). Mapping of Multicomponentsystems. J. Geol.64 533-537

[52] (Forgotson Jr. J.M. 1960). Review and classification of quantitative mapping technique. American Association of PetroleumGeologistsMemoir. 44. 83–100.

[53] Harbaugh J W and Bonham-Carter G (1970). Computer Simulation in Geology (New York:Wiley Inter. Science) pp. 575.

[54] Anderson T W and Goodman L A (1957).Statisticalinference about Markov chain; Ann. Math. Statist. 28 89–11

AUTHORS

First Author – Dinga Elvis Tita, Department of Geology, University of Buea, Cameroon. BP.63. Buea, E-mail:defttita@yahoo.co.uk.
Tel. 00237675352067

Second Author – Adrien LamireDjomeni, Department of Earth Sciences, Faculty of Sciences, University of Douala Cameroon.